Available online at www.sciencedirect.com

SCIENCE DIRECT

Cement and Concrete Research 35 (2005) 1999 – 2007

Cement and Concrete Research

Hydration characteristics of waste sludge ash utilized as raw cement material

Kae-Long Lin [a,*], Chung-Yi Lin [b]

[a] Department of Environmental Engineering, National I-Lan University, I-Lan, 26041 Taiwan, ROC
[b] Waste Minimization Division, Foundation of Taiwan Industry Service, Taipei, 198 Taiwan, ROC

Received 6 June 2005; accepted 6 June 2005

Abstract

In this study, the hydration characteristics and the engineering properties of three types of eco-cement pastes, including their compressive strength, speciation, degree of hydration, and microstructure, were studied and compared with those of ASTM type I ordinary Portland cement. The results indicate that it is feasible to use sludge ash and steel-making waste to replace up to 20% of the mineral components of the raw material of cement. Furthermore, all the tested clinkers met the toxicity characteristic leaching procedure requirements. The major components of Portland cement, C_3S (i.e., $3CaO{\cdot}SiO_2$), C_2S (i.e., $2CaO{\cdot}SiO_2$), C_3A (i.e., $3CaOAl_2O_3$) and C_4AF (i.e., $4CaO{\cdot}Al_2O_3{\cdot}Fe_2O_3$), were all found in the waste-derived clinkers. All three types of eco-cements were confirmed to produce calcium hydroxide ($Ca(OH)_2$) and calcium silicate hydrates (CSH) during the hydration process, increasing densification with the curing age. The thermal analysis results indicate that the hydration proceeded up to 90 days, with the amount of $Ca(OH)_2$ and CSH increasing. The chemical shift of the silicates, and the resultant degree of hydration, and the increase in the length of the CSH gels with the curing age, were confirmed by ^{29}Si NMR techniques. Compressive strength and microstructural evaluations confirm the usefulness of eco-cement.

Keywords: Cement; Thermal analysis; Calcium silicate hydrates (CSH); Clinker; Hydration

1. Introduction

With the increasing quantity of waste sludge and lack of landfill sites, how to dispose and reuse the sludge is becoming an important and immediate concern. In Taiwan, the annual sludge production from its 29 purification treatment plants and 22 sewage treatment plants are 160,000 tons and 180,000 tons, respectively. The annual sludge (dewatered) production from its 34 industrial wastewater treatment plants is approximately 670,000 tons.

Therefore, from the viewpoint of waste disposal, how to improve the ratio of recycled resources and how to recycle wasted resources have become very important environmental protect on subjects. In recent years, studies have been carried out by various researchers investigating the use of sludge in construction materials. The sewage sludge ash retained in filters can be deposited in controlled landfills or used in construction, sometimes even improving the properties of the building materials. Tay [1,2] has reported independently that sludge mixed with clay can be used in the production of bricks for construction use. Incineration residues such as rice husk ash [3,4] and municipal solid waste ash [5] have also been used successfully in construction. SSA has been used in mortars [6], in concrete mixtures [7,8], in brick manufacturing [9], as a fine aggregate in mortars [10], and in asphalt paving mixes. The reuse of waste in cement production mainly depends on the chemical composition of the waste. They are mainly composed of

* Corresponding author. Tel.: +886 39357400x749; fax: +886 39367642.
E-mail address: kllin@niu.edu.tw (K.-L. Lin).

0008-8846/$ - see front matter © 2005 Elsevier Ltd. All rights reserved.
doi:10.1016/j.cemconres.2005.06.008

Table 1
Chemical analysis and heavy metals of the raw materials

	IWSA	WPSA	PSSA	Ferrate	Limestone
Chemical composition					
SiO_2 (%)	12.19	54.47	63.31	3.17	7.30
Al_2O_3 (%)	43.54	29.12	15.38	1.63	1.10
Fe_2O_3 (%)	7.44	7.25	6.81	40.50	0.66
CaO (%)	2.65	0.93	1.80	5.73	62.10
MgO (%)	0.59	1.12	1.03	0.23	1.23
SO_3 (%)	3.20	0.08	1.01	0.82	0.18
Na_2O (%)	1.24	0.67	0.70	0.08	0.22
K_2O (%)	0.55	3.55	1.51	0.07	0.01
P_2O_5 (%)	1.51	ND	7.20	ND	ND
Cl^- (ppm)	315	311	105	175	ND
LOI (%)	27.09	2.78	1.25	47.59	27.20
Cu (mg/kg)	19,826	76	1321	–	–
Cr (mg/kg)	1210	1.2	16	–	–
Cd (mg/kg)	54	1.1	15.4	–	–
Pb (mg/kg)	4254	36.4	284	–	–
Zn (mg/kg)	6258	96	1084	–	–

SiO_2, CaO, MgO, Al_2O_3 and Fe_2O_3 [11]. Sludge originating from an incinerator primarily consists of SiO_2 , CaO and MgO, and has the same physical properties as the powdered minerals [12]. A feasibility test has been conducted to address the suitability of reusing sludge after a burning process as eco-cement clinkers. The potential of the process for sludge reduction, and the performance of the eco-cement paste has also been investigated. In this study, the hydration characteristics of these eco-cements and the engineering properties of their pastes, including their compressive strength, speciation and degree of hydration, were studied and compared to those of ASTM type I ordinary Portland cement (OPC).

2. Materials and methods

2.1. Clinker preparation

Waste sludge and steel slag can be recycled as a partial replacement for the raw materials of cement. A hydraulic type of cement (referred to as eco-cement) was produced using different types of sludge ash, including those from sewage water treatment, water works, and aluminum-containing industrial wastewater sludge, as well as wastes from steel works (ferrate). The chemical and mineralogical composition of the sewage sludge ash (SSA), water purification sludge ash (WSA), aluminum-containing wastewater sludge ash (ASA), and steel slag closely resembled those of silica, clay, alumina, and iron oxide, as shown in Table 1.

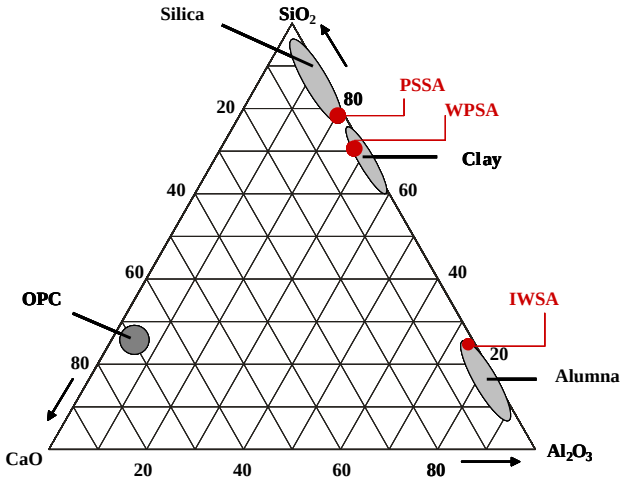

Fig. 1. The ternary diagram of the raw materials.

Table 2
Blend ratios (wt.%) of the raw materials

	ECO-I	ECO-II	ECO-III
Type of Blend			
Limestone (%)	80.12	79.97	79.43
WPSA (%)	8.69	9.72	6.18
PSSA (%)	8.51	6.84	9.29
IWSA (%)	1.00	1.50	3.00
Ferrate (%)	1.68	1.97	2.10
Modulus			
LSF	0.91	0.83	0.80
HM	2.00	1.87	1.72
SM	1.90	2.16	1.74
IM	2.11	2.10	1.79

Water purification sludge ash (WPSA), primary sewage sludge ash (PSSA), industrial wastewater sludge ash (IWSA), limestone, and ferrate were used as raw materials in the tests. The oxide composition of these raw materials, on a loss free basis, is given in Table 1. This provides the possibility, as depicted by the ternary diagram in Fig. 1, of recycling SSA, WSA and ASA as substitutes for silica, clay and alumina in raw cement. A computational model [13] was used to formulate the composition of the raw clinkers.

The raw materials were blended using three different ratios: eco-cement I, eco-cement II, and eco-cement III (eco-cement I, eco-cement II and eco-cement III referred to as ECO-I, ECO-II and ECO-III, respectively). Each of the eco-cement clinker ratios is computed, after considering the hydration modulus, $\left(\mathrm{HM}=\frac{\mathrm{CaO}}{\mathrm{SiO_2}+\mathrm{Al_2O_3}+\mathrm{Fe_2O_3}}, 1.7<\mathrm{HM}<2.3\right)$, the lime saturation factor $\left(\mathrm{LSF}=\frac{\mathrm{CaO}}{\mathrm{SiO_2}+1.18\mathrm{Al_2O_3}+0.65\mathrm{Fe_2O_3}}, 0.8<\mathrm{LSF}<0.95\right)$, the silica modulus $\left(\mathrm{SM}=\frac{\mathrm{SiO_2}}{\mathrm{Al_2O_3}+\mathrm{Fe_2O_3}}, 1.9<\mathrm{SM}<3.2\right)$, and the iron modulus $\left(\mathrm{IM}=\frac{\mathrm{Al_2O_3}}{\mathrm{Fe_2O_3}}, 1.7<\mathrm{IM}<2.5\right)$. The four unknowns are solved by simultaneous 1st order equations and the clinker composition was estimated using ASTM C150, and by checking the moduli. The blend ratios are shown in Table 2.

The burning process is summarized as follows: incinerated sewage sludge, industrial wastewater sludge and water purification sludge ashes were separated, dried and pulverized in a pretreatment process. The pretreated incinerated ash was mixed with other raw materials (e.g. ferrate) and supplements (e.g. limestone). The ground mixtures were burned in a programmable electrical furnace. The compound material was burned for 6 h at 1400 °C to form eco-

Table 3
Chemical composition of the OPC and eco-cement clinkers

	OPC	ECO-I	ECO-II	ECO-III
Composition				
SiO_2 (%)	20.04	21.14	23.11	22.53
Al_2O_3 (%)	5.35	7.55	7.24	8.32
Fe_2O_3 (%)	3.44	3.58	3.45	4.64
CaO (%)	63.16	64.55	63.17	61.18
MgO (%)	2.31	1.28	1.17	1.11
SO_3 (%)	2.03	0.38	0.41	0.45
R_2O (%)[a]	0.56	0.24	0.21	0.18
TiO_2 (%)	0.27	0.33	0.27	0.31
P_2O_5 (%)	ND	0.48	0.50	0.85
f-CaO (%)	0.23	0.30	0.30	0.20
Cu (mg/Kg)	814	3838	3326	4844
Cr (mg/Kg)	ND	ND	ND	ND
Cd (mg/Kg)	ND	ND	ND	ND
Pb (mg/Kg)	964	2114	1076	2794
Zn (mg/Kg)	2212	3128	2916	3418
Constituents				
C_3S (%)	51.01	45.15	26.74	13.98
C_2S (%)	23.21	26.55	46.08	54.05
C_3A (%)	8.21	13.95	13.35	14.20
C_4AF (%)	10.32	10.89	10.50	14.12

[a] R_2O(%): $Na_2O+0.659\ K_2O$.

Table 4
Range of ^{29}Si chemical shifts of Q^n units in solid silicates

Types of Si–O–X group	Symbol	Range (ppm)
Monosilicates	Q^0	−68 to −76
Disilicates and chain end group	Q^1	−76 to −82
Chain middle groups	Q^2	−82 to −88
Chain branching sites	Q^3	−88 to −92
Three-dimensional framework	Q^4	−92 to −129

cement clinkers. After the burning process, the resultant clinkers were allowed to cool rapidly to room temperature. The clinkers thus produced were ground in a laboratory ball mill with 3.5% per weight of gypsum to obtain the eco-cements (i. e. ECO-I, ECO-II and ECO-III in Table 3). The Blaine's surface was over 300 m^2/kg. ASTM type I ordinary Portland cement, made by the Taiwan Cement Works Inc., was used as the reference material.

2.2. Preparation approach

Three types of eco-cement clinkers prepared as above were used. Pastes using the aforementioned blends were prepared with a water to binder ratio of 0.38. $25.4 \times 25.4 \times 25.4$ mm ($1 \times 1 \times 1$ in.) test cubes were prepared according to ASTM-305, followed by a moulding process (ASTM C31-69). The specimens were then demoulded and cured in a container at 95% humidity, at 25 °C for 3–90 days. The compressive strength development of three samples of each type of eco-cement paste was measured at different ages, according to ASTMC 39-72. The leachability of the specimens was analyzed by the Toxicity Characteristic Leaching Procedure (TCLP) tests. Any composition changes and hydrates were analyzed using X-ray diffraction (XRD) techniques. The hydration of the pulverized and sieved (#300) samples was terminated at the desired testing age with acetone in a vacuum for 24 hs for further characterization.

2.3. Analyses

The following chemical and physical analyses of the OPC and the three types of eco-cement pastes were conducted at different ages:

- Unconfined compressive strength (UCS): ASTMC39-72.
- Heavy metal leachability (TCLP): SW-846-1311.

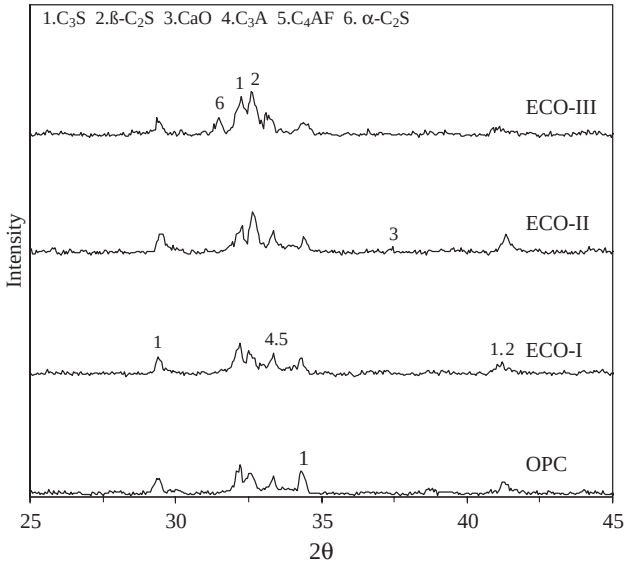

Fig. 2. XRD patterns of the OPC and eco-cement clinkers.

- Heavy metal concentration: Cd (SW846-7131A), Pb (SW846-7421), Zn (SW846-7951), Cu (SW846-7211), Cr (SW846-7191).
- Mineralogy: the XRD analysis was carried out by a Siemens D-5000 X-ray diffractometer with CuKα radiation and 2θ scanning, ranging between 10° and 70°.
- Chemical composition: the X-ray fluorescence (XRF) was performed with an automated RIX 2000 spectrometer. The specimens were prepared for XRF analysis by mixing 0.4 g of the sample and 4 g of 100 Spectroflux, at a dilution ratio of 1:10. Homogenized mixtures were placed in Pt–Au crucibles, then treated for 1 h at 1000 °C in an electrical furnace.
- Free CaO: To describe the burnability, the amount of free CaO in the clinker samples was determined by the Schlaepfer–Bukowsky titration method [14].
- Differential Thermal and Thermogravimetric Analysis (DTA/TGA): DTA/TGA analyses of the samples were performed using a Seiko SSC Model 5000 Thermal analyzer. Dry N_2 gas was used as a stripping gas. The heating rate was 0.5 °C. The samples were heated from 50 to 1000 °C.
- Chemical shift of linear polysilicate anions in CSH: ^{29}Si nuclear magnetic resonance (^{29}Si MAS/NMR).

The degree of hydration of the OPC and the eco-cement pastes, and the average length of the linear polysilicate anions in the calcium silicate hydrate (CSH) gels, primarily responsible for the strength, were analyzed by using high-resolution solid state ^{29}Si MAS/NMR techniques as follows:

The increase of diamagnetic shielding of the ^{29}Si nuclei that resulted from the degree of increasing condensation from the single tetrahedral structure of the monosilicates (Q^0) to the end groups (Q^1), to the chain middle groups (Q^2), to the layers and branching sites (Q^3), and finally to the three-dimensional frameworks (Q^4), led to well-separated and analytically useful chemical shift ranges for each type of SiO_4 unit [15,16]. That is, for the calcium silicate hydrates, the hydration products in the cement could be semi-quantified using chemical shifts in the ^{29}Si nuclei in the Si–O–X groups, for which the structures are shown below [17]:

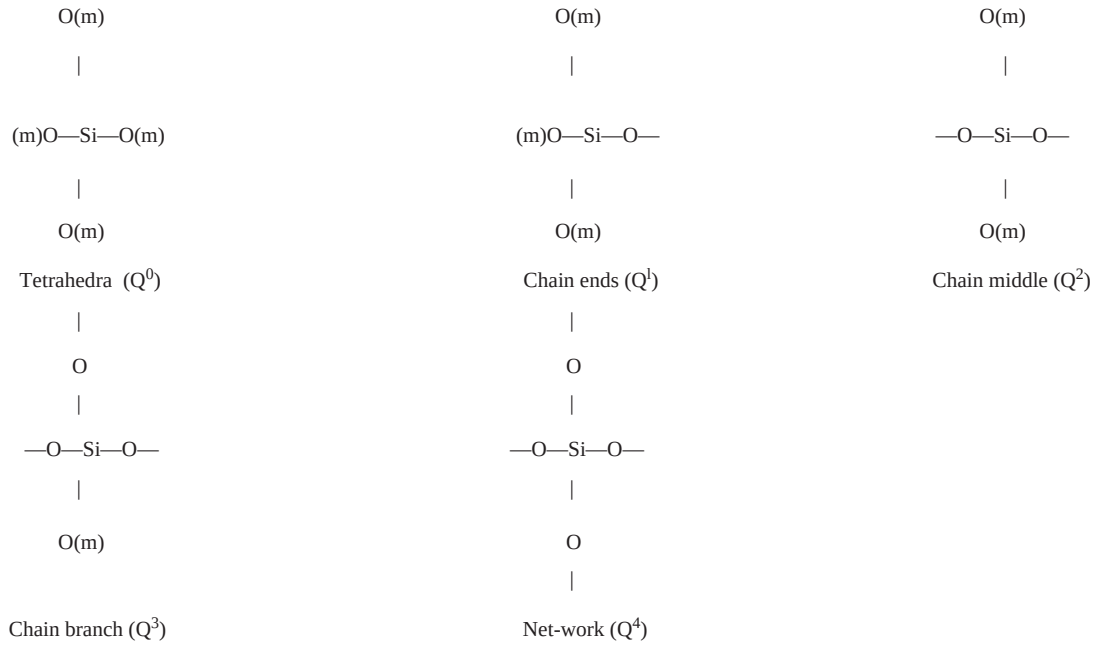

High-resolution ^{29}Si MAS/NMR spectra were recorded at 39.72 MHz on an MSL Bruker MAS/NMR-200 solid state high-resolution spectrometer, using rapid (about 3 kHz) sample spinning at the magic angle external magnetic field. The ^{29}Si chemical shifts are given relative to the primary standard liquid tetramethylsilane (TMS) in the delta-scale (the negative signs correspond to up-field shifts). The sharp ^{29}Si signal chemical shifts for the above S–O–X groups in solid silicates are summarized in Table 4.

Table 5
Heavy metal concentrations in TCLP leachates for the OPC and eco-cements

	Cu (mg/L)	Cr (mg/L)	Cd (mg/L)	Pb (mg/L)	Zn (mg/L)
OPC	ND[a]	ND[b]	ND[c]	0.72±0.02	0.33±0.01
ECO-I	ND	ND	ND	0.61±0.01	0.28±0.01
ECO-II	ND	ND	ND	0.56±0.01	0.32±0.01
ECO-III	ND	ND	ND	0.68±0.02	0.46±0.02
Regulatory thresholds	–	5.00	1.00	5.00	–

[a] Detection limits<0.020 mg/L.
[b] Detection limits<0.016 mg/L.
[c] Detection limits<0.014 mg/L.

The hydration degree (designated as $\acute{a}$) of the cement clinkers, C_2S and C_3S, can be evaluated as follows by the integral intensity of the signals at −70 ppm (Q^0) for both the hydrated cement paste and cement powders, i.e., $I^0(Q^0)$ and $I(Q^0)$, respectively [18,19]:

$$a = \left[1 - \frac{I(Q^0)}{I^0(Q^0)}\right] \times 100\%. \quad (1)$$

3. Results and discussion

3.1. Characterization of the eco-cement clinkers

The properties of the three types of eco-cement used in this study were analyzed. The results of the XRF analysis are summarized in Table 3. It is noted that SiO_2, CaO, Al_2O_3 were the primary components found in the eco-cement clinkers. Theoretical phase compositions were predicted using a modified Bogue calculation. The theoretical phase compositions are given in Table 3. The eco-cement clinkers contained 13.4–14.2% of C_3A. The other components, C_3S, C_2S, C_4AF were also present. The C_3S content in the ECO-I clinker was similar to that in the OPC. As can be seen from Table 3, the amount of free CaO were found to be 0.2–0.3%, the amount of free CaO less than 1%.

The X-ray diffraction patterns of the OPC and the eco-cement clinkers are shown in Fig. 2. Fig. 2 clearly shows the speciation in the eco-cement clinkers. The major components of OPC, C_3S (i.e., $3CaO{\cdot}SiO_2$), C_2S (i.e., $2CaO{\cdot}SiO_2$), C_3A (i.e., $3CaOAl_2O_3$), and C_4AF (i.e., $4CaO{\cdot}Al_2O_3{\cdot}Fe_2O_3$) were all presented in the ECO-ECO-I, ECO-II and ECO-III clinkers. The ECO-II produced clinkers with a greater amount of β-C_2S. The XRD pattern indicated that the amount of α-C_2S was higher for the ECO-III clinkers than for the OPC. The ECO-III clinkers contained a greater amount of α-C_2S and a smaller amount of C_3S. Increasing the P_2O_5 content lowered the C_3S/C_2S rate. The oxides, Na_2O and K_2O, the so called alkalis, are normally present in all eco-cement clinker components. The alkali content of Portland cement is usually 0.5–1.3%.

There was a high heavy metal content, including Pb, Zn, Cd, Ni, Cr and Cu, in the eco-cement clinkers, which is shown in Table 3. All the tested eco-cement clinkers met the TCLP (the toxicity characteristic leaching procedure) requirements. Their leaching concentrations also all met the regulatory thresholds (Table 5).

3.2. Compressive strength development of the OPC and eco-cement pastes

Fig. 3 shows the compressive strength of the OPC and eco-cement pastes. It can be observed from Fig. 3, that the compressive strength of the OPC and all three types of eco-cement pastes developed within the curing time (3 to 90 days). At 28-days, the strength of the ECO-I pastes was similar to that of the OPC. The graph indicates that the compressive strength development of the ECO-II paste during the initial 7 days was less than that of the OPC paste. From 28 to 90 days, the compressive strength of the ECO-II paste was greater than that of the OPC paste. The compressive strength of the ECO-III paste was lower than

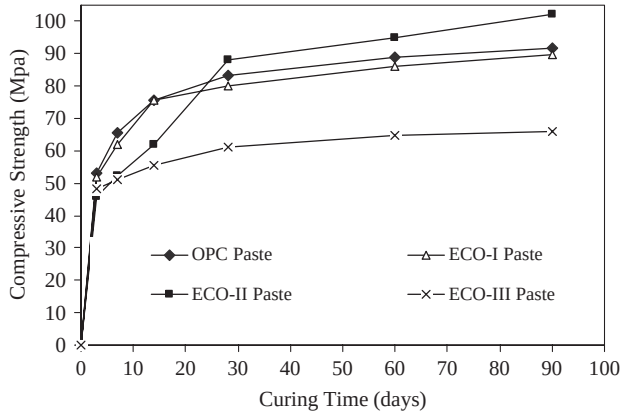

Fig. 3. Compressive strength development of the OPC and eco-cement pastes.

that of the OPC paste. A possible explanation for may be partly due to the fact that the amounts of C_3S were lower in comparison to the OPC. In addition, the higher α-C_2S, had a high value in the ECO-III eco-cement clinkers, which could make the early strength lower. Amount of P_2O_5 below 0.5 wt.% in the clinker are not effecting eco-cement quality especially strength development.

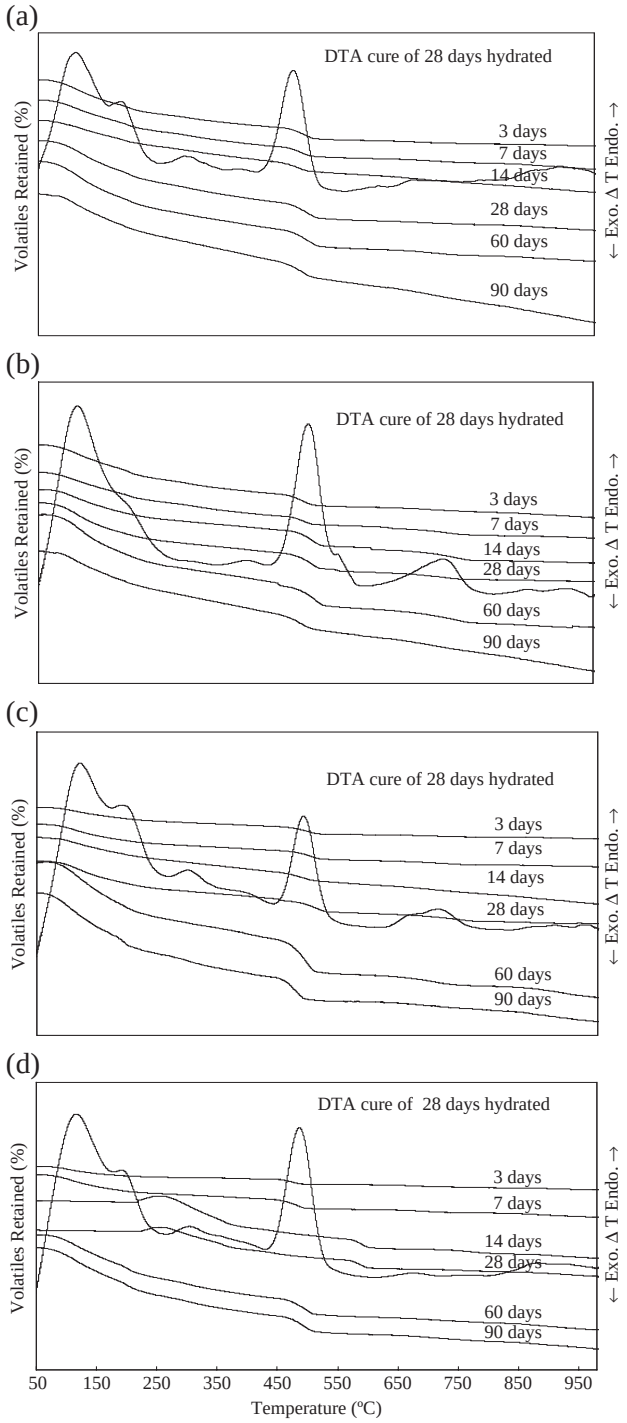

Fig. 4. The TGA/DTA curve for hydrated pastes: (a) OPC , (b) ECO-I, (c) ECO-II, and (d) ECO-III pastes.

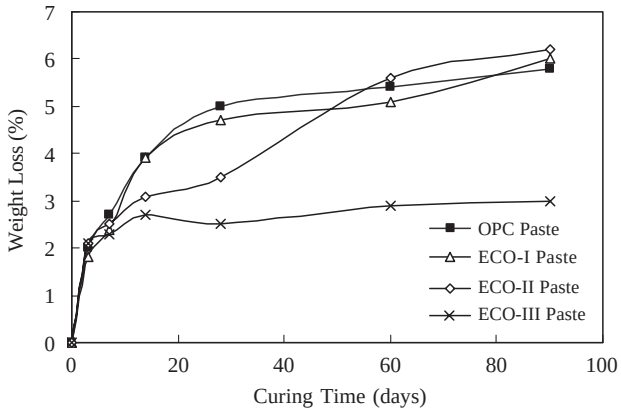

Fig. 5. $Ca(OH)_2$ mass loss during the TG analysis of the OPC and eco-cement pastes.

3.3. Differential thermal and thermogravimetric analysis of OPC and eco-cement pastes

Quantification of hydration products was made on the basis of the TG/DTA results. Fig. 4 showed the DTA/TGA results for hardened OPC and eco-cement pastes. The DTA curves for eco-cement pastes cured for 28-days have four endothermic peaks, the first at about 100–190 °C. This peak was mainly due to the decomposition of calcium silicate hydrates (CSH). The second endothermic peak was observed at about 190–250 °C and represents the decomposition of the hexagonal calcium aluminate hydrate (C_4AH_{13}). The third endothermic peak is located at about 430–550 °C represents the decomposition of calcium hydroxide ($Ca(OH)_2$). In addition, the another endothermic peak, at 650–740 °C, represents the crystalline calcium carbonate ($CaCO_3$).

Figs. 5 and 6 show the mass loss of $Ca(OH)_2$ and CSH during the TG analysis of the OPC and the eco-cement pastes, respectively. Figs. 5 and 6 indicate that as the hydration proceeded up to 90 days, the amount of $Ca(OH)_2$ and CSH increased. It can be seen that OPC and eco-cement pastes became hydrated by the production

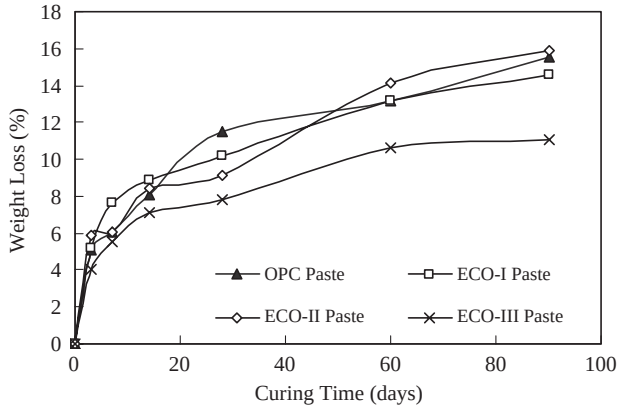

Fig. 6. CSH mass loss during the TG analysis of the OPC and eco-cement pastes.

of $Ca(OH)_2$, which increased over time up to 90 days. As hydration proceeded, the amount of CSH increased with the curing time. The results show a more rapid hydration in the control specimen during the early ages, which is related to the higher amounts of available C_3S and C_2S, which caused a change in the environmental conditions early on.

Fig. 5 shows that the formation of $Ca(OH)_2$ phases in the ECO-II paste increase between 60 days and 90 days, but this occurred later in the OPC paste. The rate of CSH development in the ECO-II paste was also faster from 60 days to 90 days. Figs. 5 and 6 indicate that the ECO-III pastes had less CSH and $Ca(OH)_2$ than did the OPC pastes, at all stages of hydration. Since a lower endothermic effect corresponds to a lower activation energy, these results confirm that the $Ca(OH)_2$ crystallinity was low at later ages.

3.4. NMR analysis of OPC and eco-cement pastes

Fig. 7 resents the ^{29}Si MAS/NMR spectra of the hydrated samples of OPC pastes at various stages. Fig. 7 shows the absorption peaks of the hydrated OPC paste, which appeared at −71.5, −81.5 and −89.5 ppm. We can see that the amount of Q^0 species decreased with the curing time. This is linked to an acceleration of the hydration with curing time, the Q^0 species being transformed into the Q^1 and Q^2 types. Table 6 clearly shows that the amount of Q^1 and Q^2 became greater with the hydration time. It is known that the CSH formed by the hydration of calcium silicates is generally dominated by Q^1 sites or has abundant Q^1 and Q^2 sites. The ratio of silicone sites in the hydrated products Q^2/Q^1, also rises after the mechanical activation of the eco-cement.

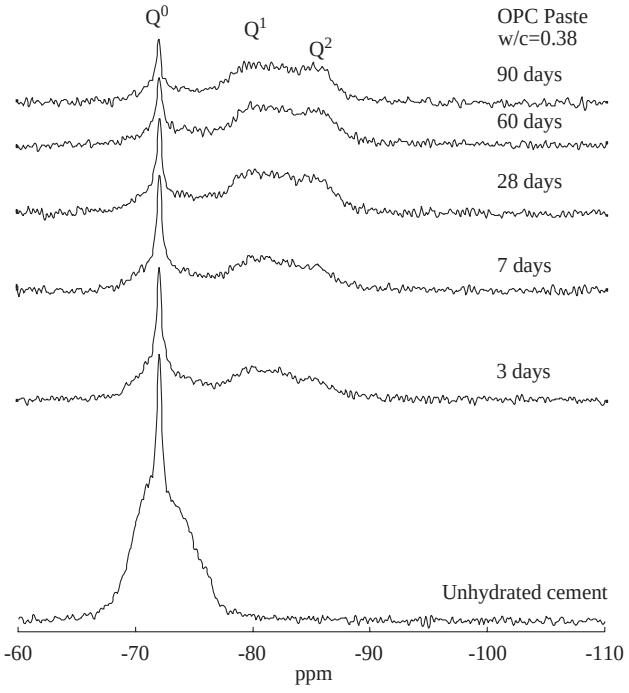

Fig. 7. ^{29}Si MAS/NMR spectra of hydrated OPC paste.

Table 6
^{29}Si NMR analysis for OPC and eco-cement monoliths at different age

Sample	Age (days)	^{29}Si NMR integral intensities of Q^n			Degree of hydration (%)
		Q^0	Q^1	Q^2	
OPC paste					
	3	61.8	23.9	14.3	38.2
	7	52.5	28.1	19.4	47.5
	14	47.7	30.8	21.5	52.3
	28	48.7	30.5	20.8	51.3
	60	35.4	39.1	25.5	64.6
	90	34.4	38.9	26.7	65.6
ECO-I paste					
	3	64.5	25.1	10.3	35.5
	7	56.1	27.5	16.4	43.9
	14	49.8	30.7	19.5	50.2
	28	49.0	28.7	22.3	51.0
	60	33.3	40.7	26.0	66.7
	90	33.4	40.0	26.6	66.6
ECO-II paste					
	3	65.7	20.7	0.119	34.3
	7	59.7	24.4	0.159	40.3
	14	50.3	29.0	0.207	49.7
	28	40.9	34.6	0.245	59.1
	60	37.3	36.3	0.265	62.7
	90	32.3	39.7	0.280	67.7
ECO-III paste					
	3	74.9	15.3	9.8	25.1
	7	68.6	18.8	12.6	31.4
	14	61.1	21.8	17.1	38.9
	28	53.4	25.0	21.5	46.6
	60	46.4	30.5	23.1	53.6
	90	38.3	33.3	28.3	61.7

These and the other results are summarized in Table 6. Table 6 indicates the hydration degree of the OPC pastes and the eco-cement pastes up to 90 days. The hydration degree of OPC increases with time, up to 90 days. The ECO-III pastes also showed lower hydration degree values at all ages of hydration. The main reason for this is that the amount of α-C_2S caused the degree of hydration in the ECO-III paste to decrease more than that of pure cement.

4. Conclusions

In this study, the hydration characteristics and the engineering properties of three types of eco-cement pastes were investigated. From the studies carried out, the following conclusions can be drawn:

1. The leaching concentrations of all three types of eco-cement clinkers met the regulatory thresholds.
2. In the XRF analysis we note that SiO_2, CaO, Al_2O_3 were the primary components found in the eco-cement clinkers. The C_3S content in the ECO-I clinkers was similar to that in the OPC.

3. The compressive strength of OPC and all three types of eco-cement pastes developed with the curing time. In addition, the higher α-C_2S, had a high value in the ECO-II eco-cement clinkers, which could make the early strength lower.
4. Amount of P_2O_5 below 0.5 wt.% in the clinker are not effecting eco-cement quality especially strength development.
5. Thermogravimetric analysis results indicate that as the hydration proceeded up to 90 days, the amount of $Ca(OH)_2$ and CSH increased.
6. The MAS/NMR spectra of the hydrated samples make it clear that the amount of Q^1 and Q^2 became greater with hydration time.
7. The results indicate that it is feasible to use sludge ash and ferrate waste to replace up to 20% of the mineral components of the raw materials of cement.

References

[1] J.H. Tay, Sludge ash as filler for Portland cement concrete, J. Environ. Eng. Div. ASCE 113 (1987) 345–351.

[2] J.H. Tay, W.K. Yip, Sludge ash as lightweight concrete material, J. Environ. Eng. ASCE 115 (1989) 56–64.

[3] P.K. Mehta, Properties of blended cements, cements made from rice husk ash, J. Am. Concr. Inst. 74 (1997) 440–442.

[4] P.K. Mehta, D. Pirtz, Use of rice husk to reduce temperature in high strength mass concrete, J. Am. Concr. Inst. 75 (1978) 60–63.

[5] J.I. Bhatty, J.K. Reid, Compressive strength of municipal sludge ash mortars, ACI Mat. 86 (1989) 394–400.

[6] J. Monzó, J.M. Payá, V.A. Borrachero, Use of sewage sludge ash (SSA)–cement admixtures in mortars, Cem. Concr. Res. 26 (1996) 1389–1398.

[7] J.H. Tay, Bricks manufactured from sludge, J. Environ. Eng. ASCE 113 (1987) 278–283.

[8] J.H. Tay, K.Y. Show, Clay blended sludge as lightweight aggregate concrete material, J. Environ. Eng. Div. ASCE 117 (1991) 834–844.

[9] J.E. Alleman, N.A. Berman, Constructive sludge management: biobrick, J. Environ. Eng. Div. ASCE 110 (1984) 301–311.

[10] J.I. Bhatty, J.K. Reid, Compressive strength of municipal sludge ash mortars, ACI Mater. 86 (1989) 394–400.

[11] C.G. Kim, H.S. Lee, T.I. Yoon, Resource recovery of sludge as a micro-media in an activated sludge process, Adv. Environ. Res. 7 (2003) 629–633.

[12] H. Belevi, M. Langmeier, Factors determining the element behavior in municipal solid waste incinerators: 2. Laboratory experiments, Environ. Sci. Technol. 34 (2000) 2507–2512.

[13] J. Majling, D.M. Roy, The potential of fly ash for cement manufacture, Am. Ceram. Soc. Bull. 72 (1993) 77–81.

[14] A. Altun, Influence of heating rate on the burning of cement clinker, Cem. Concr. Res. 29 (1999) 599–602.

[15] J. Hjorth, ^{29}Si MAS/NMR studies of Portland cement components and effects of microsilica on the hydration reaction, Cem. Concr. Res. 18 (1988) 788–798.

[16] G. Engelhardt, D. Michel, High-Resolution Solid-State NMR of Silicates and Zeolites, John Wiley & Sons, New York, 1987.

[17] H. Justnes, I.M. Bjoergum, J. Krane, T. Skjetne, NMR—a powerful tool in cement and concrete research, Adv. Cem. Res. 30 (1990) 105–113.

[18] C.K. Lin, J.N. Chen, C.C. Lin, An NMR, XRD and EDS study of solidification/stabilization of chromium with Portland cement and C_3S, J. Hazard. Mater. 56 (1997) 21–34.

[19] K.S. Wang, K.L. Lin, Z.Q. Huang, Hydraulic activity of municipal solid waste incinerator fly ash slag blended eco-cement, Cem. Concr. Res. 31 (2001) 97–103.